Supplementary Figure S1

a

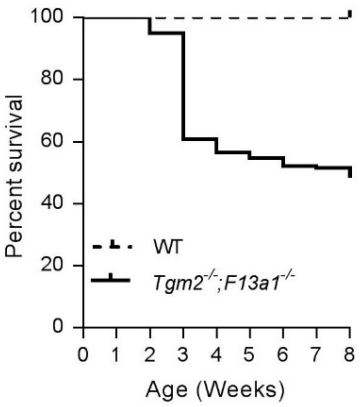

b

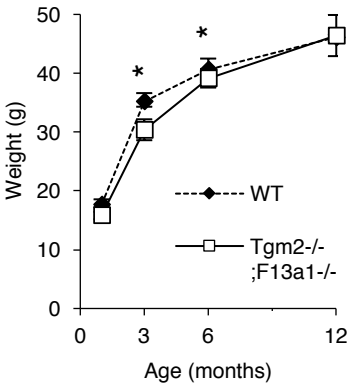

c

	Genotype	Body weight/ Tibia length	Body weight/ Tibia width
		g/mm	g/mm
1 mo	WT	0.27±0.004	3.62±0.1
1 mo	*Tgm2*$^{-/-}$;*F13a1*$^{-/-}$	0.25±0.01	3.45±0.1
3 mo	WT	0.43±0.01	5.59±0.2
3 mo	*Tgm2*$^{-/-}$;*F13a1*$^{-/-}$	0.38±0.01**	5.42±0.1

d

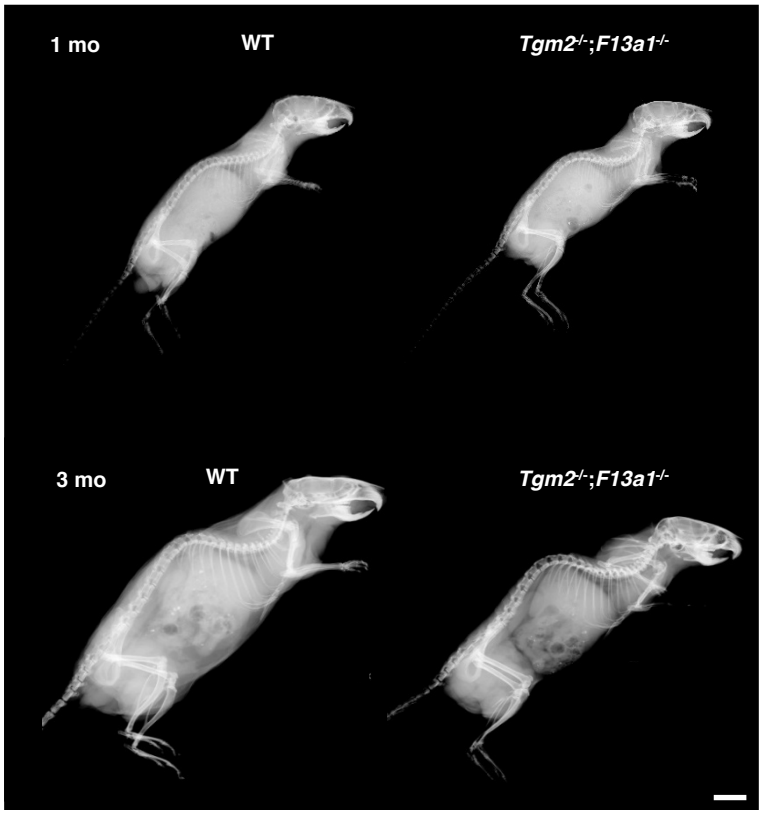

e

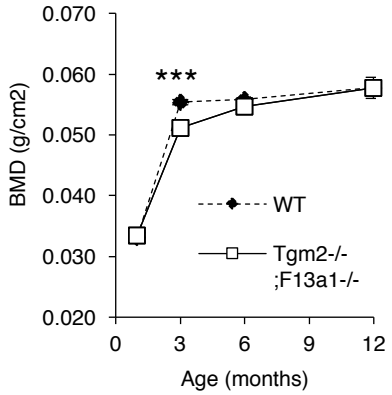

Supplementary Figure S1. Survival and gross phenotype of *Tgm2*$^{-/-}$;*F13a1*$^{-/-}$ double-null mice. (**a**) Kaplan-Meier survival curve showing increased lethality in *Tgm2*$^{-/-}$;*F13a1*$^{-/-}$ mice; 51.5% of male mice were lost by 4 weeks of age (161 male mice counted). (**b**) Body weight measurements of the surviving mice show that *Tgm2*$^{-/-}$;*F13a1*$^{-/-}$ are normal weight at 1 month mice but have lower body weight at 3 and 6 months which normalizes again 1 year age. n=6-14. (**c-d**) Measurements of tibia lengths and their normalization to body weight show that mice are smaller only at 3 months and not at 1 month. n=6. (**d**) X-ray images of representative WT and *Tgm2*$^{-/-}$;*F13a1*$^{-/-}$ mice at 1 month and 3 month age. *Tgm2*$^{-/-}$;*F13a1*$^{-/-}$ mouse appears normal size at 1 month and smaller at 3 month age. (**e**) Bone mineral density (BMD) measurements of WT and *Tgm2*$^{-/-}$;*F13a1*$^{-/-}$ mice up to 1 year age. Data shows that WT mice reach their adult BMD at 3 months, but that *Tgm2*$^{-/-}$;*F13a1*$^{-/-}$ mice do not. However, normal BMD is reached at 6 month age. n=6-15. *p<0.05, ** p<0.01, ***p<0.001. Scale bar: 1 cm.

Supplementary Figure S2

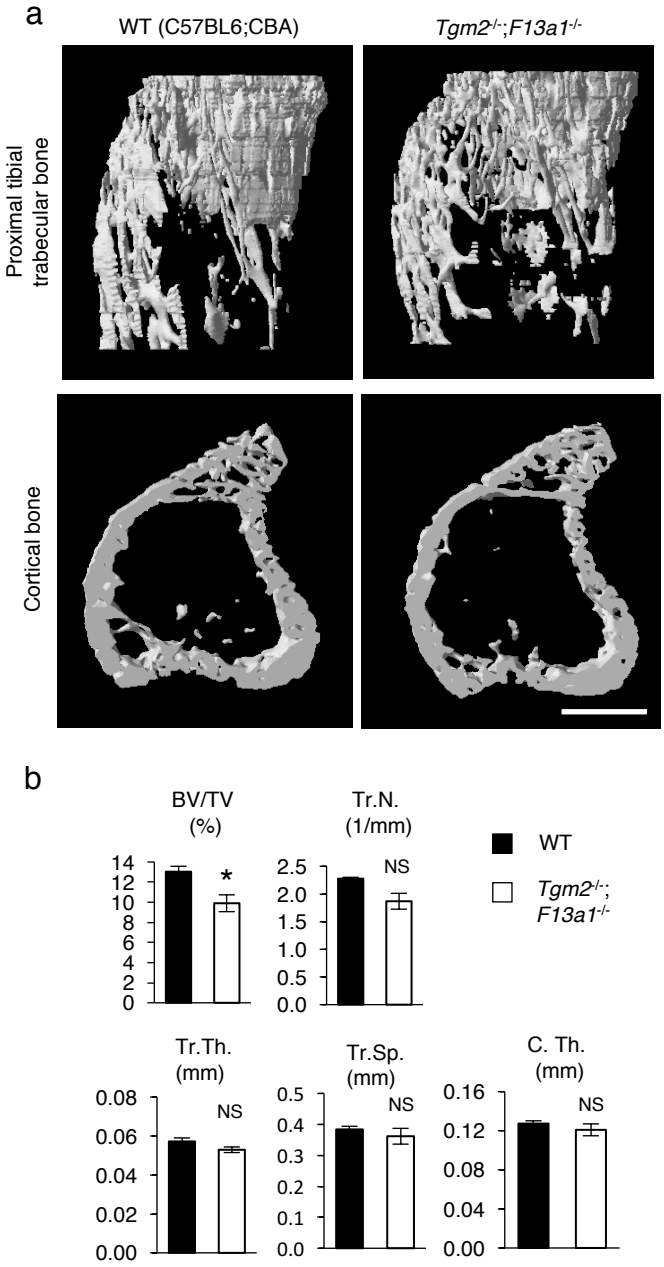

Supplementary Figure 2. Micro-computed tomography (μCT) analyses of bone parameters of proximal tibial trabecular bone and cortical bone of 1 month old WT and *Tgm2*$^{-/-}$;*F13a1*$^{-/-}$ mice. (**a**) No trabecular bone loss or cortical thinning was visible in 1 month old *Tgm2* $^{-/-}$;*F13a1* $^{-/-}$ mice. (**b**) Quantified μCT parameters of bone shows only decreased mineralized bone volume over tissue volume (BV/TV). Other parameters: trabecular number (Tr.N.), trabecular thickness (Tr.Th.), trabecular spacing (Tr.Sp.) and cortical thickness (C.Th) show no significant difference between WT and in *Tgm2*$^{-/-}$;*F13a1*$^{-/-}$ mice. n=4 for each group. *p<0.05, NS; not significant. Scale bar: 500 μm (a)

Supplementary Figure S3

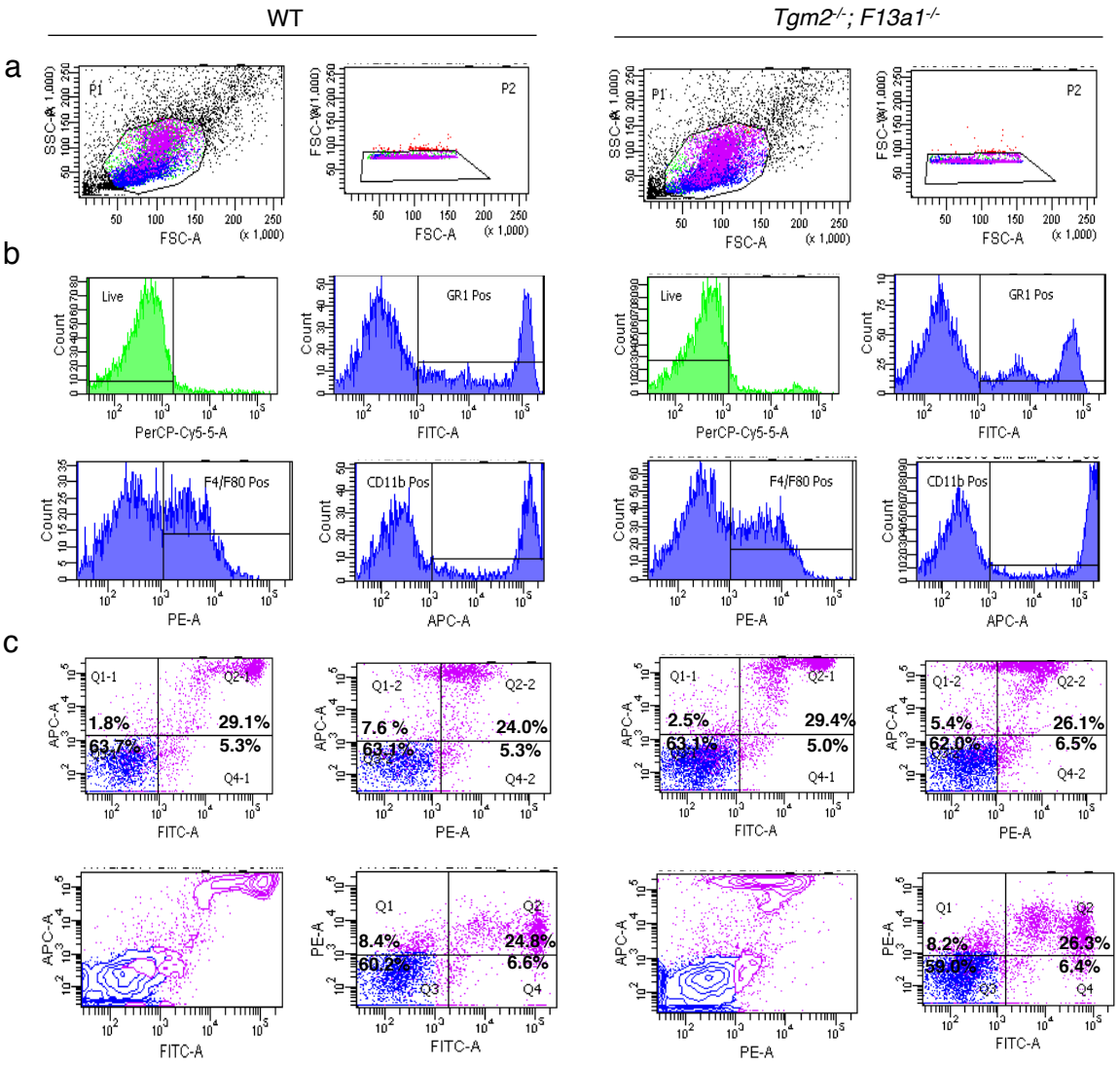

Supplementary Figure S3. No alterations in bone marrow myeloid lineage cell levels in 3 month old *Tgm2*$^{-/-}$;*F13a1*$^{-/-}$ mice. (**a**) Representative flow cytometry plots using FACSDIVA software. Dead cells were excluded by selecting all live cells from the Side-scatter (SSC) / Forward-scatter (FSC) plot which showed no differences in cell populations in general. (**b**) Histograms depict cell counts of Gr-1 (FITC), CD11b (APC) and F4/80 (PE) positive cells showing no differences in monocytes, neutrophils or eosinophils and macrophage levels in the marrow. (**c**) Percentages of 3-color single tube of bone marrow cells suspension is indicated on each two color combination plot of *Tgm2*$^{-/-}$;*F13a1*$^{-/-}$ cells and WT cells showing no significant differences. Compensation controls for each fluorophore were included in each experiment. Sample n=3 per genotype.

Supplementary Figure S4

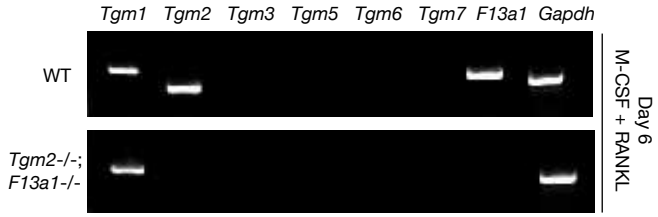

Supplementary Figure S4. Expression of TG family members in WT and *Tgm2*$^{-/-}$;*F13a1*$^{-/-}$ in osteoclasts isolated from 2 month old mice. RT-PCR analyses of TG family members demonstrate the presence of *Tgm1*, *Tgm2*, and *F13a1* in mature osteoclasts.

Supplementary Figure S5

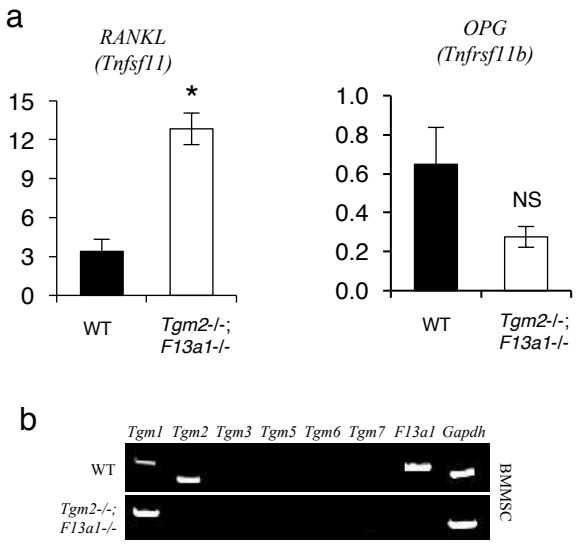

Supplementary Figure S5. qRT-PCR and RT-PCR analyses of RANKL (*Tnfsf11*), OPG (*Tnfrsf11b*) *Tgm* family members in bmMSCs isolated from 2 month old mice. (**a**) Quantification shows dramatic and significant increase in RANKL (*Tnfsf11*), decrease (not significant) in OPG in *Tgm2*$^{-/-}$;*F13a1*$^{-/-}$ cells. *p<0.05. NS; not significant. n=3. (**b**) Analysis of mRNA expression of TG family members show the presence of *Tgm2, F13a1* and *Tgm1* in bmMSCs in WT cells and upregulation of *Tgm1* in *Tgm2*$^{-/-}$;*F13a1*$^{-/-}$ cells. RT-PCR image represents data from 2 separate cell culture experiments.

Supplementary Figure S6

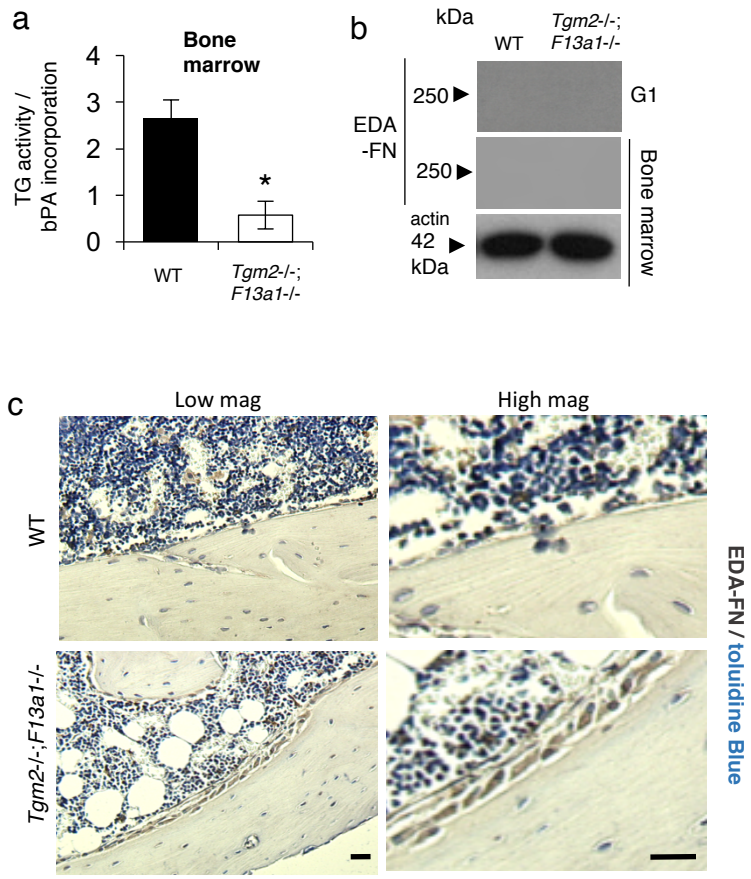

Supplementary Figure S6. EDA-FN and TG-activity in the bone marrow of 3 month old mice *Tgm2*$^{-/-}$;*F13a1*$^{-/-}$ mice. (**a**) TG-activity assay, performed using biotinylated pentylamine as a probe, shows significant decrease in TG activity in bone marrow. NS; not significant. *p<0.05, n=3. (**b**) Western blot analysis of EDA-FN in the G1-extract of bone and in flushed bone marrow show no EDA-FN in either material. The actin blot is the same as in Figure 6c as analysis was done at the same time and from same samples. Western blot image is representative of 2 blots from 3 mice. (**c**) Staining of bone sections for EDA-FN (cellular FN) (brown)(counterstained with toluidine blue) shows EDA-FN production in osteoblasts. The presence of adipocytes in the marrow is evident. Scale bars: 200 μm.

Supplementary Figure S7

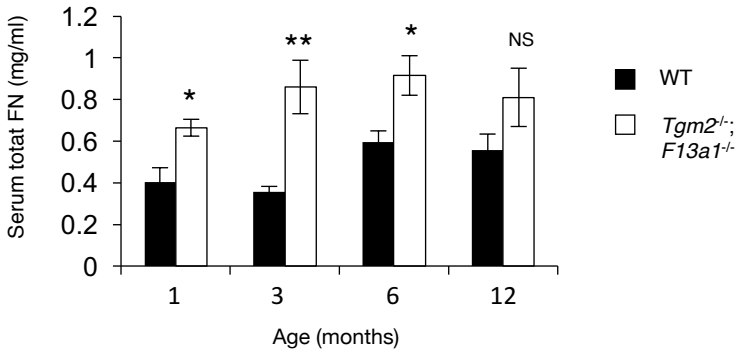

Supplementary Figure S7. Circulating pFN levels in *Tgm2*$^{-/-}$;*F13a1*$^{-/-}$ mice. Plasma (pFN) levels are significantly increased in double-null mouse sera at 1, 3 and 6 months age. One year old mice showed no significant differences. NS; not significant. *p<0.05, ** p<0.01, n=6-7.